AUTOMATIC IMAGE PROCESSING SYSTEM FOR NUCLEAR FILM DETECTORS

By

CARLOS EMILIO ZARATE, Licenciado en Ciencias Fisicas

A Thesis

Submitted to the Faculty of Graduate Studies

in Partial Fulfilment of the Requirements

for the Degree

Master of Science

McMaster University

April 1980

AUTOMATIC IMAGE PROCESSING SYSTEM FOR NUCLEAR FILM DETECTORS

MASTER OF SCIENCE (1980)
(Physics)

MCMASTER UNIVERSITY
Hamilton, Ontario

TITLE: Automatic Image Processing System for Nuclear Film Detectors

AUTHOR: Carlos Emilio Zarate, Licenciado en Ciencias Fisicas
(Universidad de Buenos Aires)

SUPERVISOR: Dr. T. J. Kennett

NUMBER OF PAGES: vi, 52

ABSTRACT

A system to process automatically nuclear film detectors was developed by interfacing a commercial television camera to a computer and analyzing the two level images of white objects on a dark background.

Two analysis methods were used; it is concluded that they have different ranges of application. For intermediate to high fluencies (> 100 impacts/mm^2) the antitransformation of the white line length distribution function obtained throughout a raster scan provides results with uncertainties smaller than the statistical fluctuations of the hole density in the film. For fluencies down to 20 impacts/mm^2 a direct image analysis gives more accurate results in reasonably short times. The limiting factor for very low fluencies is the resolution of the television camera.

ACKNOWLEDGEMENTS

I am deeply indebted to my supervisor, Dr. T.J. Kennett, for his warm encouragement and help throughout the course of this work. I also would like to express my appreciation to K. Chin for his assistance with the debugging of the system.

Finally, I thank Dr. T. Timusk for his advice and Mrs. H. Kennelly for typing the final manuscript.

TABLE OF CONTENTS

LIST OF FIGURES

CHAPTER 1

INTRODUCTION

The detection of alpha activity is of considerable interest in several important industrial activities such as uranium prospecting and the monitoring of radon and aerosol activity in uranium mines.

In the area of uranium prospecting, the detection of near surface soil radon anomalies has been used for a number of years as an exploration tool in the search of buried uranium mineralization[1].

In uranium mining it is desired to monitor the dosages associated with inhaling radon daughter products which present the greatest danger to the mine workers[2]. The maximum permissible exposures set by government agencies are extremely low, e.g., 4 WLM (Working Level Month)[3] per year, which corresponds approximately to 15 mrem/year.

Both kinds of work require the measurement of low level alpha activity which is independent of short term variations and can be conducted in many locations. The range of alpha particles in material media is very short, typically some 50 μm, hence detection by conventional means requires some form of sample preparation in which the radioactive element is extracted from the bulk. Even after this is accomplished,

long periods of counting are required to handle a large number of low activity samples. The capital and operational costs of conventional alpha-sensitive detector systems make the obvious parallel counting approach extremely expensive, ruling out its use for industrial applications.

Several types of film are now being used for detection of heavy particles by making use of the radiation damage they produce[5,6,7]: the zones damaged by radiation of an exposed film have a much higher etching rate than the bulk, producing pits or, if the etching time is long enough, holes in the film. If coloured emulsion is used, development results in pinpoint holes on a near opaque medium.

For detection of alpha particles, a red cellulose nitrate film produced by Kodak[18] is commonly used. If high contrast images are desired, a green Kodak Wratten W-40 filter can be employed since its optical transmission properties are complementary to those of the Kodak film.

The size of the etched holes in the film depends on the developing procedure but it is typically of the order of 3 to 15 μm[9,10], requiring a microscope of at least 50 power for their counting. The dose is simply proportional to the number of holes in the processed film.

A measurement of optical density might appear to be an attractive alternative to manual track counting, which is a costly and time consuming procedure. However, R. Countess[11] found that in exposing films to standard ^{239}Pu sources the

optical density is neither a linear function of track density nor reproducible and that the optical density is significantly different from unexposed film only when high alpha fluencies (> 400 alphas per square millimeter) are used. More recently, Quagish et al.[10] and Luck[9] have developed etching techniques which allow, for normal particle incidence, the determination of the particle energy within 50 keV for energies between 3 and 6 Mev. Interposition of an absorber can extend the range of this spectroscopic technique to higher energies[12]. This means that, if in addition to track counting, size measurements are desired, manual processing of the films becomes even more expensive for large scale applications.

The purpose of this work is to develop an automatic system to both count and classify etched holes by their size in a film. Through minimal operator intervention, high cost effectiveness is sought with a minimization of human errors. With such a development the processing of a large number of of films or even the study of flux distribution ("hot spots") within one plate could be readily realized.

CHAPTER 2

SYSTEM IMPLEMENTATION

1) General considerations:

Automatic scanning systems consist of three components: a scanning apparatus, a computer to process the image and ancillary electronics to interface these subunits and produce the necessary timing and control signals (handshaking).

The scanning equipment has to be tailored to the needs of the job to be done. To scan by specimen motion[12] using a fixed detector provides a resolution only limited by the optics employed and permits a very large area to be scanned but requires a special and relatively complex mechanical system and is extremely slow, typically 10 h/cm^2. To process a large number of samples in a reasonable time an electro-optical scanning system is necessary. A commercial television camera, while not offering a very large number of picture elements (pixels), provides a fast reliable solution to this problem[13].

Several commercial equipments [14,15] are available to digitize and store a TV image in real time with intensity encodement of 6 or 8 bits per pixel, but their speed and memory size makes them complex and expensive while still requiring the use of a computer to process the image; random

access is inherently slow and sequential data transfer is impossible except for computers with a large available memory. As the image to analyse consists of bright shapes on a dark background, only two levels are really required to describe it, if some method to properly adjust the discrimination level is found. This allows a more efficient memory utilisation and, consequently, image storage directly into the computer without the need of an external memory.

An alternative way to store the whole two level image is to transfer to the computer only the distribution of line lengths of say bright spots produced throughout a raster scan. By subsequent antitransformation, the number and size of the tracks can be estimated. This method has problems discriminating shapes other than very simple ones, does not provide any information on the spatial distributions of them and still requires adjustment of the discrimination level; however, it is easier to implement in real time, requires no memory for image storage and uses much simpler and faster software.

Due to the above considerations, it was decided to construct an interface circuit to transfer a two level image to the computer memory, produce the line length distribution using software and compare the results obtained from both methods.

2) Digitization timing considerations:

Commercial TV cameras[16] scan the image field 30 times a second using horizontal raster scan. To avoid flickering, the image is scanned twice in that time, with each line of one frame positioned between two consecutive lines of the other (interlacing). Vertical and horizontal syncronisation signals are added to the video signal to allow receiver syncronisation.

In some cameras, the horizontal and vertical oscillators are independent (random interlacing). In more expensive models, the vertical frequency is an exact half multiple of the horizontal one (2:1 interlacing); also, usually in this type of camera the horizontal synchronisation pulses are sent even during the vertical synchronisation.

In both types, the horizontal scanning frequency is 15750 Hz. This means that for each field, 525 horizontal lines are scanned. Of these, at least 18 are used for the vertical syncronisation, which leaves a usable maximum of 507 lines. Usually cameras do not have a useful image scan of more than 480 lines.

The horizontal scanning period is 63.5 µs. Of this time, approximately 5.5 µs are used for horizontal syncronisation (to allow flyback) and zero reference level (front and back porch). This results in a total image time of 58 µs per line. To preserve the 4/3 aspect ratio, a line must be

divided into 640 pixels, i.e., the sampling rate must be approximately 11 MHz.

3) Computer data input:

A Nova 2 minicomputer from Data General Corporation operating under real time disk operating system (RDOS) [17] was used but similar considerations can be applied to any other computer which can be interfaced.

Using RDOS the operator can transfer to and from the magnetic disk unit data and programs in several computer languages. Non-standard input-output (I/0) operations can be included in high level languages using user defined subroutines in assembler or low level language.

Nova computers can handle I/0 operations in basically three ways:

1) Standard data transfer: the current program specifically executes the I/0 operations. The program loops until the flags of the addressed device indicate to the processor that the device is ready to transfer data.

2) Program interrupt: the processor has special lines which allow interruption of the current program sequence by the peripheral devices; then, it services the interrupt requests by jumping to the interrupt service routine and, upon completion, reassumes normal program operation.

3) Data channel transfer: handling data transfer between external devices and memory under program control requires

one interrupt (if used) plus the execution of several instructions for each word transferred. To allow greater transfer rates the processor contains a data channel through which a device, at its own request, can gain access to memory using a minimum of time.

The computer memory is used to store the two level image derived from the video camera. The discrimination level which makes the black/white decision is set by an analog to digital converter under computer control.

As each computer word has 16 bits, 16 pixels can be stored per word. Due to available memory size, a full field cannot be stored in the computer. Instead of reducing the field size to meet the memory restrictions, only one kind of frame is read while skipping data from the other. This procedure renders an image of 240 lines rather than the potential 480. To preserve the aspect ratio, the sampling rate must be only one half of the one for a full field, thereby producing an image of 256 points per line. Due to optical and electronics limitations, the image created in this way is more accurate than one obtained by reducing the full interlaced field until the memory requirements are the same for both.

For an image obtained reading only one kind of frame, real time input requires a data transfer rate of 5.5/16 = .344 MHz, i.e., an input each 2.9 μs. This rules out the

use of standard data input; only a data channel transfer with either buffering or look ahead signals (because of the data channel latency time) would permit the storage of an image in real time. With a full 512 pixel line, only a high speed data channel can handle the data transfer rate. As this introduces a significant complication in the interface design and makes the system highly computer dependent, this approach was not followed.

Owing to the above considerations, only part of the image can be read during one frame time. The simplest way to accomplish this while still retaining a relatively fast data transfer rate is to read a 16 pixel segment for each line within a frame; after the frame is finished, the next column is read; this gives a time of at least 63.5 μs between data input requests to the computer to transfer information. As this time is of the order of the time necessary to service an interrupt and return to normal program execution, standard data transfer is used, with the computer exclusively devoted to the television interface during the time it takes to read and transfer one complete frame. During this period program interrupts are disabled in order to avoid missing image data and reduce latency.

In figs. 2.1 and 2.2 the data input sequence for a frame (no interlacing) and a complete field (with interlacing) are shown.

Figure 2.1

16 bit segment sequence for an image of 240 lines by 256 columns with no interlacing.

COLUMN / LINE	0-15	16-31		224-239	240-255
0	0	240		3360	3600
1	1	241		3361	3601
2	2	242		3362	3602
3	3	243		3363	3603
238	238	478		3598	3838
239	239	479		3599	3839

Figure 2.2

16 bit segment input sequence for a full interlaced image of 480 lines by 512 columns.

LINE \ COLUMN	0-15	16-31	...	480-495	496-511
0	0	480		14400	14880
1	240	720		14640	15120
2	1	481		14401	14881
3	241	721		14641	15121
...	...	...	...	...	...
478	239	719		14639	15119
479	479	959		14879	15359

CHAPTER 3

ELECTRONICS

The purpose of the electronics is to interface the TV camera to the computer. A block diagram indicating the salient functions performed is shown in fig. 3.1.

The TV signal is sent to a synchronisation seperator and to an analog comparator whose reference input is controlled by the computer via a digital to analog converter.

The syncronisation separator works basically in the same way as in a commercial TV receiver: a differentiator for horizontal syncronisation and an integrator with a comparator to detect the vertical syncronisation signal. After a vertical syncronisation pulse is detected, the first horizontal syncronisation pulse is fed to the frame identifier which classifies each frame as odd or even and generates the vertical and horizontal clock pulses; for a 65K bit image, they are sent only for frames of one kind; for full interlacing (256K bit image), for alternating types of frames. The vertical clock pulses are fed to a counter which establishes the position of the column to be read.

An image reading sequence is as follows: when the computer sends a START pulse, the frame identifier and the counters of number of white pixels are cleared and the column

Figure 3.1

Electronics block diagram. The computation time necessary to obtain the optimum discrimination level is substantially reduced by counting the image number of white pixels using hardware rather than software.

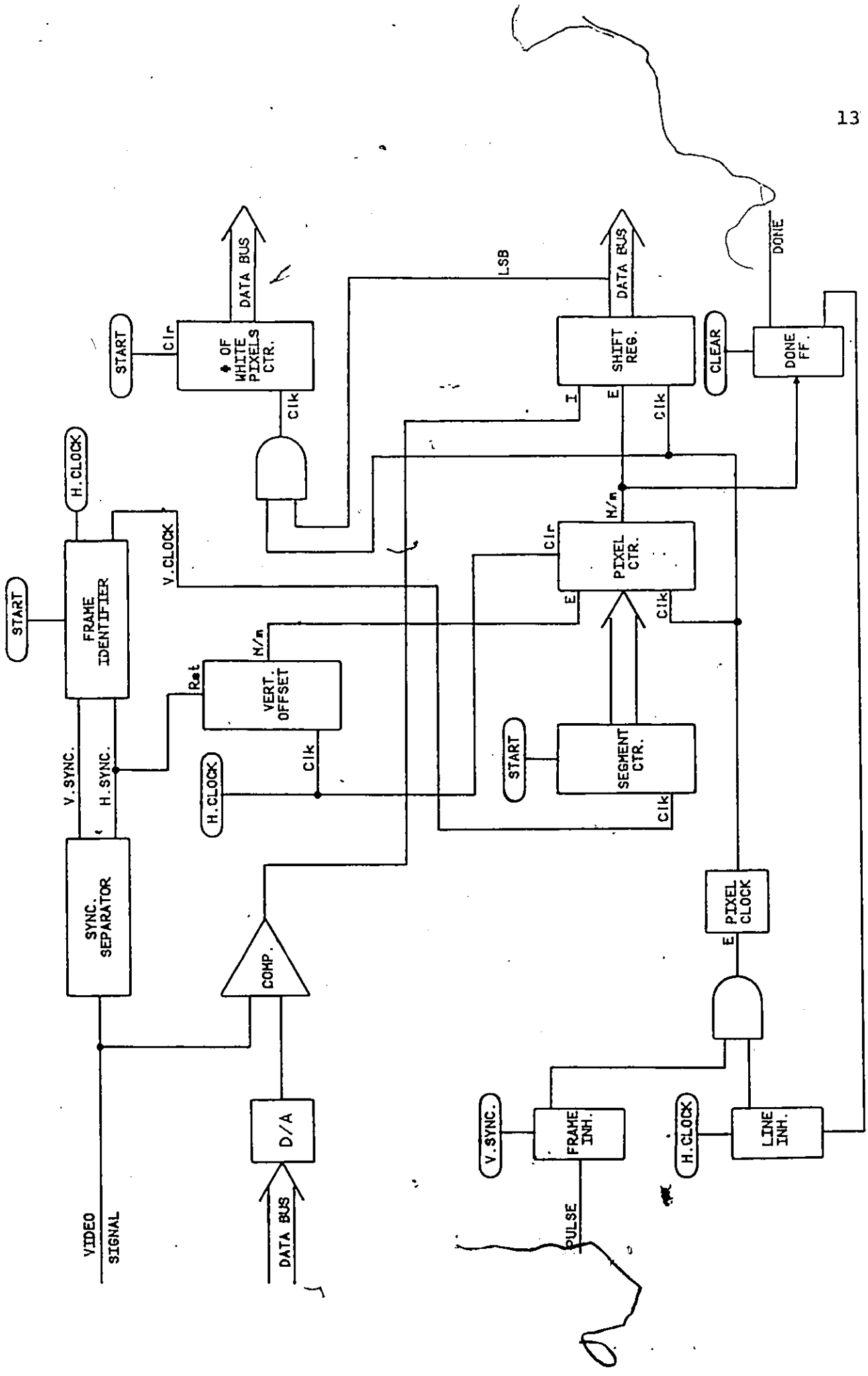
VIDEO SIGNAL
DATA BUS
D/A
COMP.
SYNC. SEPARATOR
V.SYNC.
H.SYNC.
FRAME IDENTIFIER
START
H.CLOCK
V.CLOCK
VERT. OFFSET
N/n
Rst
Clk
H.CLOCK
OF WHITE PIXELS CTR.
START
Clr
DATA BUS
Clk
LSB
SHIFT REG.
I
E
Clk
DATA BUS
PIXEL CTR.
Clr
N/n
E
Clk
SEGMENT CTR.
START
Clk
CLEAR
DONE FF.
DONE
PIXEL CLOCK
E
V.SYNC.
FRAME INH.
PULSE
H.CLOCK
LINE INH.

counter is reset to the value of the first column.

Once an allowed type of frame is received the frame identifier enables the system and the process of reading a column begins: the vertical offset counter is clocked by the horizontal clock pulses and keeps the pixel counter disabled until it reaches zero. Then, the pixel clock decreases the value of the pixel counter; when it reaches zero, sixteen pixels are read into a shift register and the number of elements with values above the reference (white pixels) is added to the counter of white pixels. Then the DONE flag is set and the pixel clock disabled. Once the computer reads the data it sends a CLEAR pulse; the next horizontal clock pulse again enables the pixel clock.

The sequence continues until the computer has read the desired number of segments. Then it sends a signal, PULSE, which disables the pixel clock until a new allowed frame is received. When this happens, the segment counter is incremented and the process of reading a column is repeated until the whole image has been transferred to the computer. As neither interrupt nor data channel lines have been used, the computer only needs to enable the interrupt request line to continue normal operation.

CHAPTER 4

SOFTWARE

1) Programming language:

The ease of debugging software when high level compiler language is employed prompted the use of Basic. Nova Extended Basic (18) is an interpreter language which allows disk transfer and can handle I/O operations and assembler subroutines in general through "Call" statements.

Assembler arrays and subroutines:

Basic stores simple precision variables in floating point notation using two words per variable; this fact makes bit operations extremely slow and produces inefficient memory use for integer numbers storage. Because of this, one assembler array was defined to store the image and another one for histograms manipulation. Also, as the total length of the software exceeded the available memory space, it was divided into several blocks concatenated using "Chain" instructions which erase the current program and variables, load the new program and run it. A third assembler array was defined to pass global variables from one program block to the next; these assembler arrays are not erased when a new program is run but are permanently attached to the interpreter. "Call" subroutines were created to gain access from

Basic (read and write) to these assembler arrays; one more subroutine was added to read and/or erase a bit directly from the image array.

Another shortcoming of Nova Basic is that it is only an interpreter language: its operation is slow compared to compiler languages. The problem is compounded by the fact that, as in almost every high level language, I/O operations to non-standard peripheral devices have to be handled by assembler subroutines like "Call". Thus, assembler subroutines were created to read the whole image into the computer, to display it on a monitor screen, and to obtain the line length distribution.

2) Image aspect ratio:

There is only one parameter of the system which must be tailored to a particular TV camera: as the vertical to horizontal scanning speed ratio varies slightly from camera to camera, the image will be stretched in one direction, e.g., converting circles into ellipses. One way to correct this is to adjust the interface clock frequency until the image proportions are equal to those of the object. Instead, following the approach of maximum simplicity of operation, the vertical coordinate is transformed linearly:

$$y \rightarrow \alpha y \qquad (4.1)$$

A program was developed to determine α as the axes ratio of the digitized image of a circle. Once it is obtained, it is included in the analysis programs and it is not modified until the camera is changed.

3) Data analysis:

The software must perform three basic functions which are:

a) Determination of object-background separation level,

b) Object counting and error, and

c) Display and control.

Fig. 4.1 indicates the principal functions and shows their interrelation.

a) Object-background separation:

The image is made up of bright shapes on a dark background; the most straightforward way to discriminate is by level separation, i.e., any pixel of intensity larger than a threshold value is considered white:

$$P_{ij} = \frac{1}{2} [1 + sg\ (U_{ij}-V)] \qquad (4.2)$$

where

U_{ij} is the pixel intensity at the position i,j,

V is the threshold value, and

P_{ij} is the assigned value to the pixel.

The main problem is then to determine the optimum separation level V_o. This is accomplished using the static mode

Figure 4.1

Software general block diagram. The operator controls the order of execution of the analysis programs by means of computer switches.

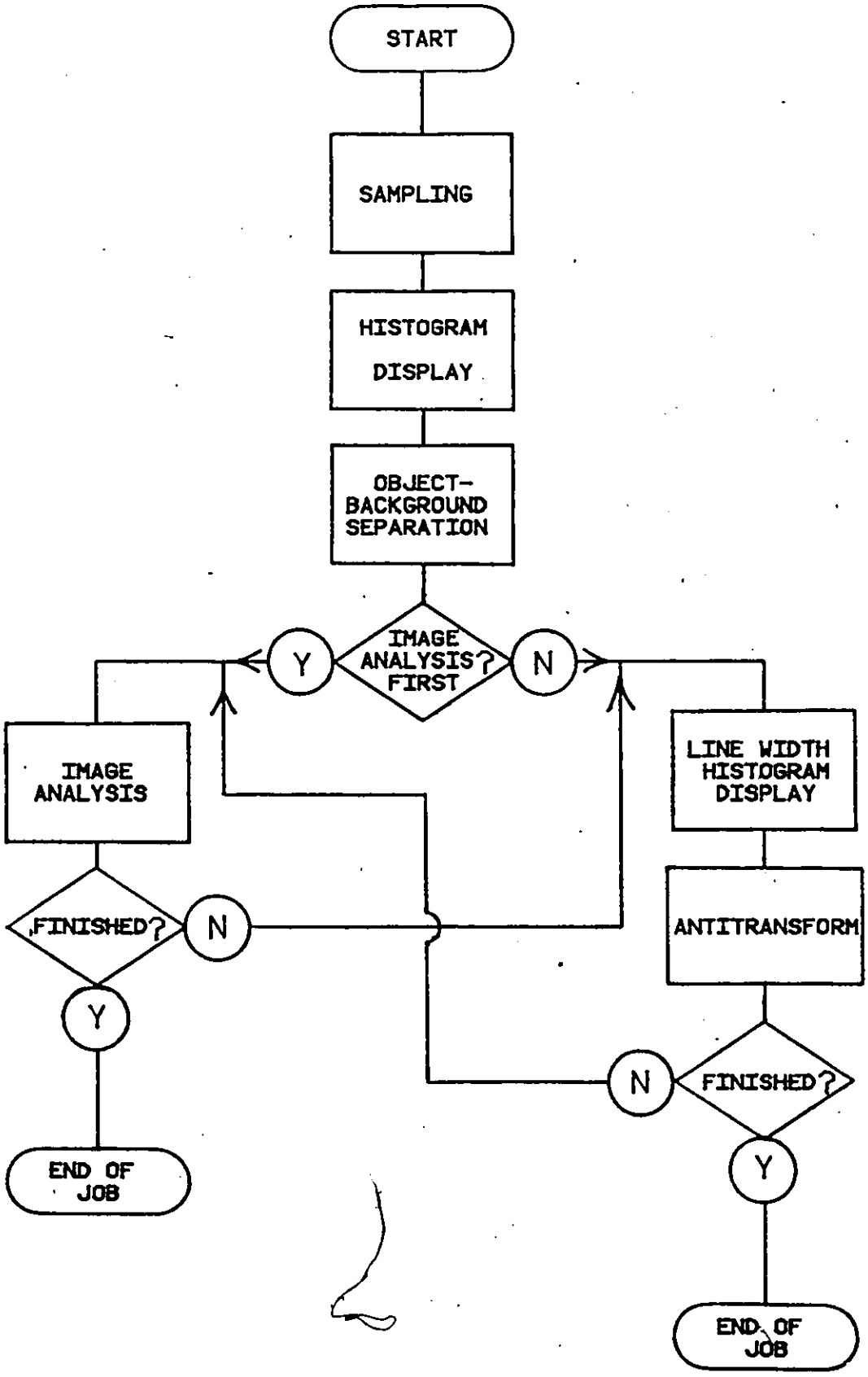
START
SAMPLING
HISTOGRAM DISPLAY
OBJECT-BACKGROUND SEPARATION
IMAGE ANALYSIS FIRST?
Y
N
IMAGE ANALYSIS
FINISHED?
N
Y
END OF JOB
LINE WIDTH HISTOGRAM DISPLAY
ANTITRANSFORM
N
FINISHED?
Y
END OF JOB

method [18], in which one first computes the intensity distribution (i.e., the gray level density function) of the whole picture and tacitly assumes the observed distribution to be bi-modal. One then identifies the intensity level corresponding to the valley point in the distribution as the threshold. The program "Sample" (see fig. 4.2) constructs a distribution function with

$$H(V) = \sum_{\text{image}} P_{ij}(V) \quad . \tag{4.3}$$

By properly selecting the lowest V value V_1, the highest V_2, and the step size a smooth function can be constructed in a reasonably short time such that

$$H(V_1) = N \text{ (total number of pixels)}$$

$$H(V_2) = 0.$$

The intensity distribution of the image is obtained by differentiating H

$$h(V) = dH(V)/dV \quad . \tag{4.4}$$

As an example fig. 4.3 shows the distribution function of an image composed by objects of total area S_1 and light level U_1 on a background of area S_2 and intensity U_2, with $U_1 > U_2$. Due to local variations in illumination and film thickness, electronics bandwidth, scanning spot size, shape edge and optical sharpness, etc., the edges of the function

Figure 4.2

"Sample" block diagram. The program checks the smoothness of the histogram by comparing the present number of white pixels with the value obtained from a quadratic interpolation from previous points.

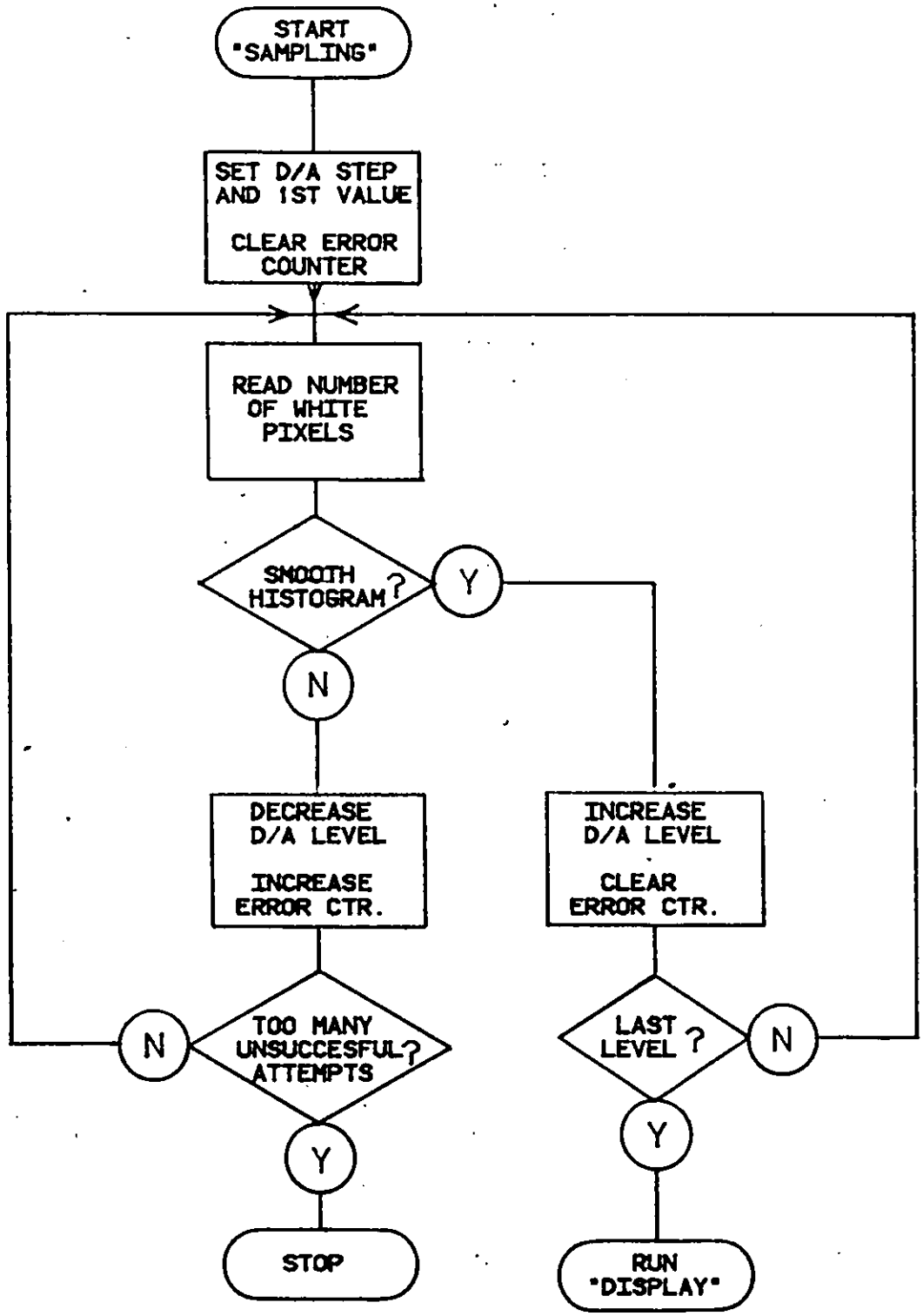
START "SAMPLING"
SET D/A STEP AND 1ST VALUE
CLEAR ERROR COUNTER
READ NUMBER OF WHITE PIXELS
SMOOTH HISTOGRAM?
Y
N
DECREASE D/A LEVEL
INCREASE ERROR CTR.
INCREASE D/A LEVEL
CLEAR ERROR CTR.
TOO MANY UNSUCCESFUL ATTEMPTS?
N
Y
LAST LEVEL ?
N
Y
STOP
RUN "DISPLAY"

Figure 4.3

Number of white pixels as a function of the discrimination level for a bimodal image. The best object-background separation level is near the inflexion point of the curve, i.e., the minimum of the grey level density function.

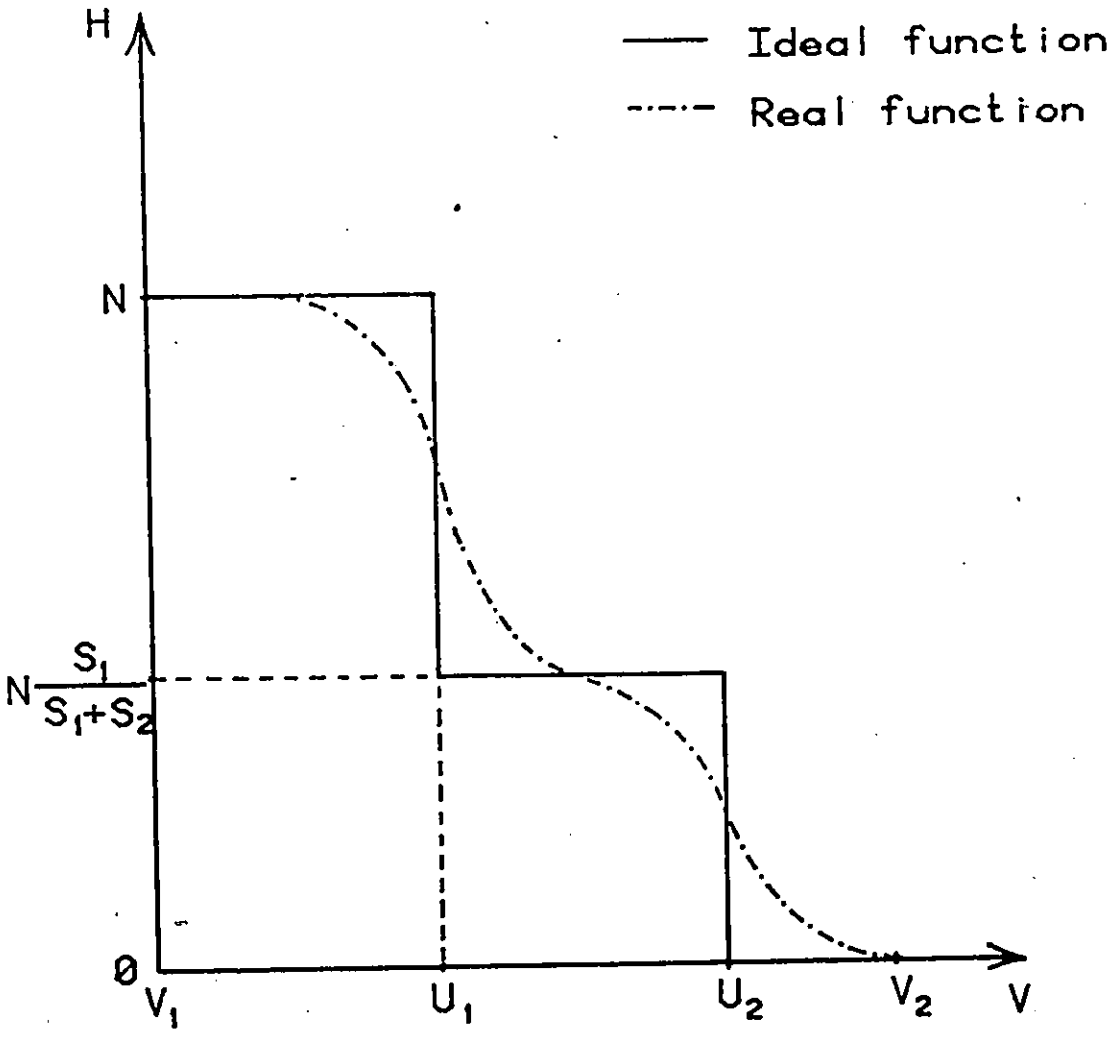
H
Ideal function
Real function
N
N S1/(S1+S2)
0
V1
U1
U2
V2
V

are rounded; the same considerations apply to h(V). The best object-background separation level will be at the minimum of h(V) between the background and object peaks, i.e., the position at which a change in V produces a minimum change in the total number of white pixels.

"Peak" (see fig. 4.4) calculates V_o by a quadratic fit to log ($|h(V)| + 1$) around a smooth minimum of h(V) between both maxima. Once V_o is calculated, the image is reread with that discrimination level. The position of computer switches allows the operator to execute one or both object counting programs.

a) Object counting and error:

As stated previously, two methods of data processing are to be explored: i) image analysis, and ii) line length distribution followed by antitransformation. Both of these approaches presuppose that the shapes of the figures to be analysed are circles; while the first method can obviously be modified to analyse different shapes, the second one can only be adapted to very simple geometrical shapes.

i) Image analysis (see fig. 4.5): the image is scanned until one point of a figure is found. To obtain the figure boundary, a versor is defined with a direction rotated 90° counterclockwise from the scanning direction and with origin in the boundary point; if the element to which it points does not belong to the figure, the versor is rotated clock-

Figure 4.4

"Peak" block diagram. A triangular smoothing function is used to find an approximate minimum of h(V).

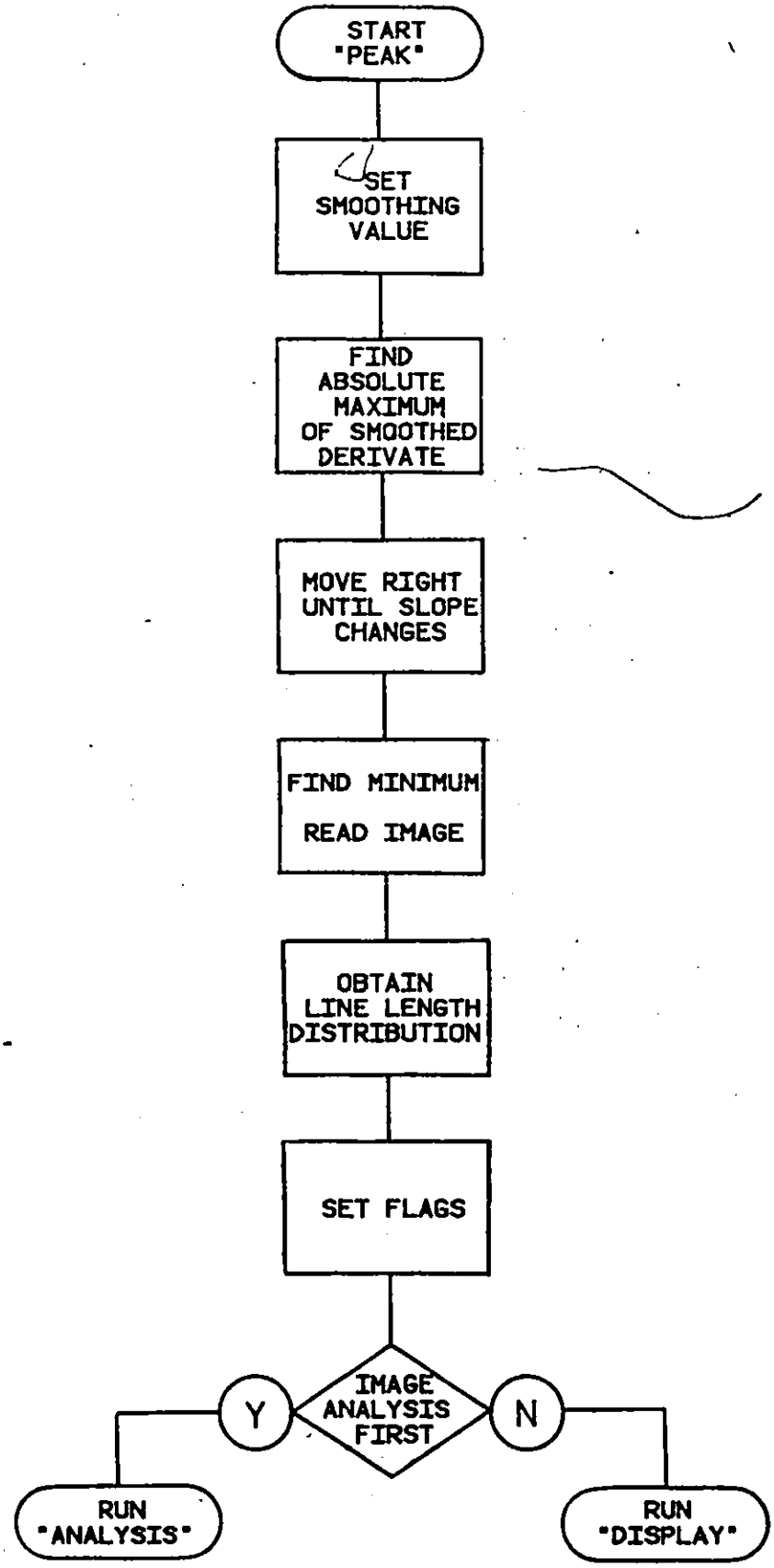
START
"PEAK"
SET
SMOOTHING
VALUE
FIND
ABSOLUTE
MAXIMUM
OF SMOOTHED
DERIVATE
MOVE RIGHT
UNTIL SLOPE
CHANGES
FIND MINIMUM
READ IMAGE
OBTAIN
LINE LENGTH
DISTRIBUTION
SET FLAGS
IMAGE
ANALYSIS
FIRST
Y
N
RUN
"ANALYSIS"
RUN
"DISPLAY"

Figure 4.5

Image analysis block diagram. Each figure in the image is individually processed and erased after its parameters have been calculated. The program ends when the image has been completely erased.

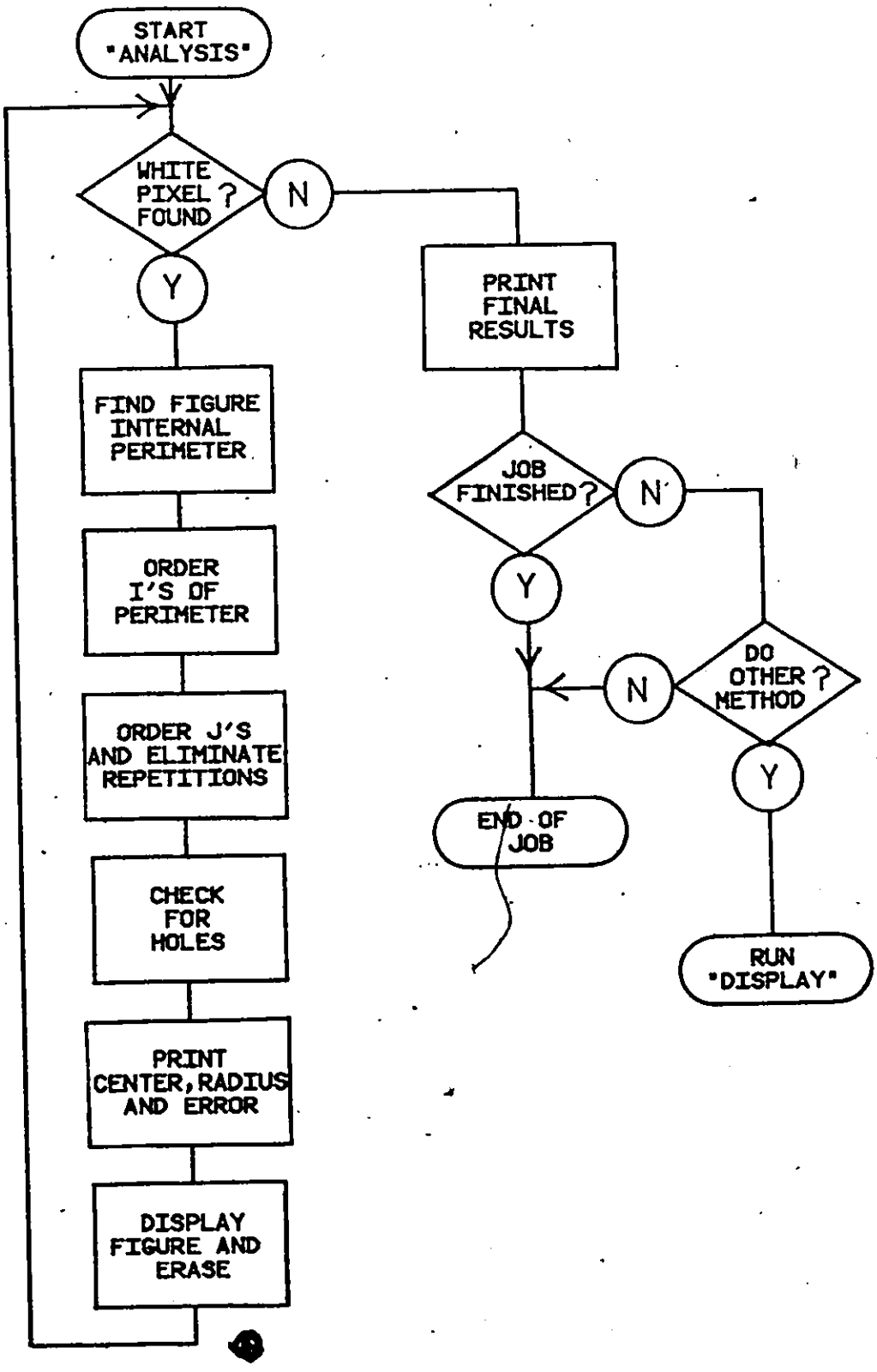
START "ANALYSIS"
WHITE PIXEL ? FOUND
N
Y
FIND FIGURE INTERNAL PERIMETER
ORDER I'S OF PERIMETER
ORDER J'S AND ELIMINATE REPETITIONS
CHECK FOR HOLES
PRINT CENTER, RADIUS AND ERROR
DISPLAY FIGURE AND ERASE
PRINT FINAL RESULTS
JOB FINISHED?
N
Y
DO OTHER ? METHOD
N
Y
END OF JOB
RUN "DISPLAY"

Figure 4.6

An example of the operation of the routine to extract a figure from the background by finding its internal boundary. The numbers indicate the order in which the border elements are obtained. The letters refer to the search sequence for the versors centered in each boundary point. Dashed and full arrows indicate unsuccessful and successful attempts respectively.

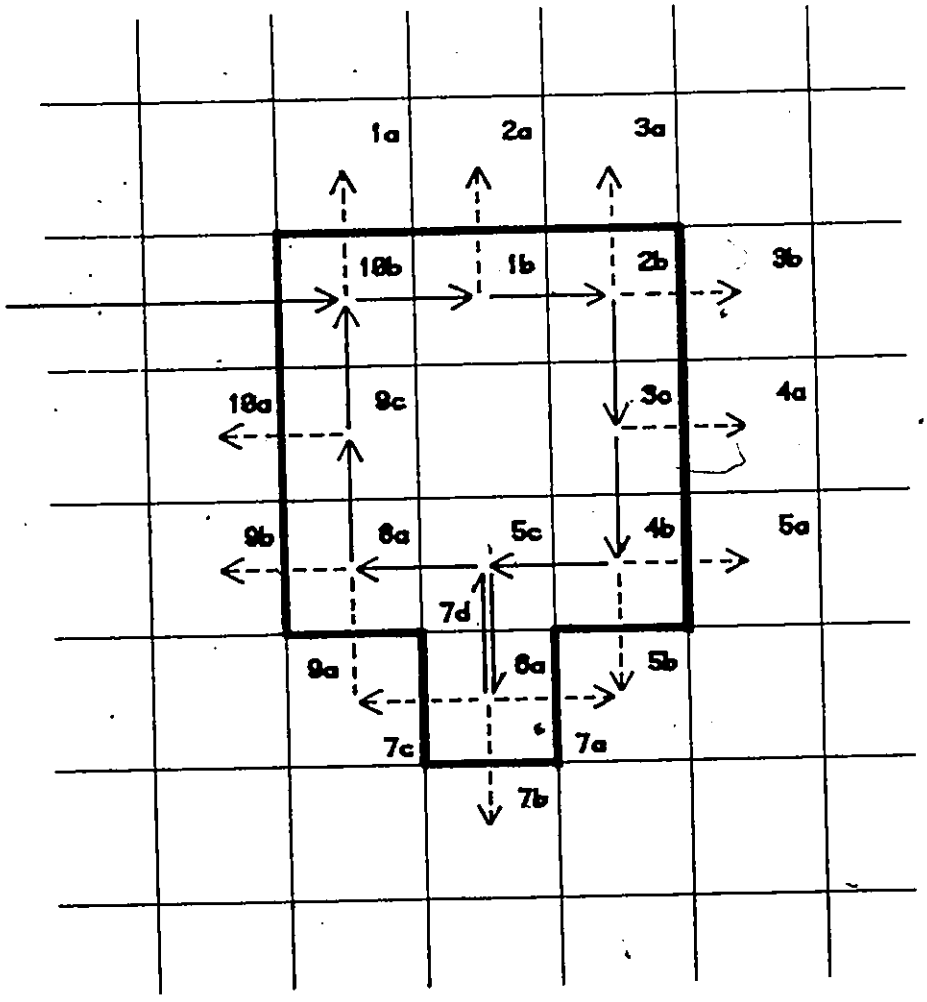
1a
2a
3a
1bb
1b
2b
3b
9c
3c
4a
9b
8a
5c
4b
5a
7d
9a
8a
5b
7c
7a
7b

wise 90° and the operation is repeated until the cursor points to a figure element, even if it is the previous point to the actual one. The versor is then rotated 90° counterclockwise; the new point, which belongs to the boundary, is taken as the new origin and the sequence is repeated until the whole boundary has been obtained in a clockwise motion. Figure 4.6 shows an example of boundary search sequence using this routine.

The same figures can be extracted from an image using a cursor which moves on the figure external boundary in 45° clockwise steps, but this routine gives the external boundary; if no background properties are desired, the internal boundary is a more convenient form of the result.

The boundary points B_{ij} are reordered and the figure parameters are calculated. Defining

$$\sum_{\text{bulk}} \equiv \sum_{i_{\text{bound}}} \sum_{j_\ell(i)}^{j_r(i)} \tag{4.5}$$

where $j_\ell(i)$ and $j_r(i)$ are the values of the leftmost and rightmost, respectively, positions of a white pixel segment in the i-th line (there may be more than one for the same i value):

Area:
$$A = \sum_{\text{bulk}} P_{ij} = \sum_{\text{bulk}} 1 \quad \text{(if there are no holes)} \tag{4.6}$$

Radius:
$$R = \sqrt{A/\pi} \tag{4.7}$$

X_{center}: $$X = \frac{1}{A} \sum_{bulk} P_{ij} i \qquad (4.8)$$

Y_{center}: $$Y = \frac{1}{A} \sum_{bulk} P_{ij} j \qquad (4.9)$$

The error is calculated using a simple physical property: for a given surface, the shape with the smallest moment of inertia with respect to its center of mass is a circle. Thus

Error: $$E = k'(I-I_c)R/A^2 \qquad (4.10)$$

where I is the figure moment of inertia, I_c is the moment of inertia of a circle of the same area, k' is a scaling constant and R/A^2 is a normalizing factor. Solving for I_c

$$E = k[2\pi/A^2-(1-1/A)] \qquad k = k'/2\pi \qquad (4.11)$$

i.e., the error depends on the shape and not on the size of the figure. To give an idea of the values involved, for an ellipse

$$E = k/2\,(\beta+1/\beta-2) \quad \beta \text{ axes ratio} .$$

For two tangent circles of the same radii

$$E = k/2 .$$

While a figure is being processed it is erased; the program then scans the image until a new figure is found. The

algorithm is repeated until the image is completely erased. Display subroutines can show on a CRT display, if desired, the erased figures, the present image to process and the last processed figure.

ii) Line length distribution antitransform: as the line length distribution function is the composition of several circles

$$f(\ell) = \sum_{D} g_D(\ell) \tag{4.12}$$

where f(l) is the total distribution function of line length l and $g_D(\ell)$ is the distribution function of a circle of diameter D:

$$g_D(\ell) = \mathrm{Re}[(D/\ell)^2 - 1]^{-1/2} \tag{4.13}$$

In order to calculate the diameters in formula 3.12 a set of n linearly independent functions generated with diameters D_j, $j = 1,\ldots,n$ was used to describe the distribution space. Thus, formula 3.12 can be written as

$$f(\ell) = \sum_{j} p_j g_{D_j}(\ell) \tag{4.14}$$

where p_j is the number of circles of diameter D_j in the image. But f(l) is made discrete by the system, i.e.

$$f(\ell) \rightarrow f_i$$

where f_i can be approximated by

$$f_i = \int_{(i-1)E}^{iE} f(\ell)\,d\ell \qquad (4.15)$$

where E is the pixel width. If $g_{D_i}(\ell)$ is truncated in the same way.

$$g_{ij} \equiv \int_{(j-1)E}^{jE} g_{D_i}(\ell)\,d\ell = (D_i^2 - \ell^2)^{1/2}\Big|_{(j-1)E}^{jE} \qquad (4.16)$$

eq. 3.12 is reduced to a matricial form

$$f_i = \sum_j g_{ij} p_j \qquad (4.17)$$

or, in matrix notation

$$\underline{F} = \underline{\underline{G}} \cdot \underline{P} \,. \qquad (4.18)$$

Defining m as the maximum i for which $f_i \neq 0$, it can be seen the eq. 3.17 is trivial for all the values of i>m, i.e., $p_j = 0$ for all $D_j > Em$.

By selecting a proper set of vectors such that n = m, eq. 3.18 can be solved

$$\underline{P} = \underline{\underline{G}}^{-1} \cdot \underline{F} \,. \qquad (4.19)$$

The linear independence insures that $|G| \neq 0$, i.e., G^{-1} exists.

In our case, D_j were selected as

$$D_j = jE \qquad j = 1, 1...,m \ . \tag{4.20}$$

To compare the results of the antitransformation with those of the image analysis and obtain an estimate of the error, image simulations were generated with circles of several radii and center positions and analysed using both methods. It was observed that, for $R > 1.6$, the results obtained from the antitransformation are the actual values within a multiplying constant that depends on the fractional part of the radius and is independent of its integer part. If this constant is made also dependent on the integer part of the radius, the number of circles can be counted down to $R > 1$. Below that value, the line length distribution becomes so center-dependent that a very large number of circles is necessary to obtain a reasonable estimate of its value, destroying the usefulness of the method to count low exposures.

It was also observed that the accuracy in the value of the radius of a group of circles can be improved considerably by taking the ratio of the group maximum to the value for the adjacent larger radius.

"Antitransform" (see fig. 4.7) obtains m, generates $\underline{\underline{G}}$, calculates $\underline{\underline{G}}^{-1}$ and, with it, $\underline{P}$ and, using the conclusions from the image simulation, groups the values, calculates the mean radii, normalizes the number of circles for each group and prints the result.

Figure 4.7

Antitransformation block diagram. This method gives accurate results for fluencies neither high enough for optical dosimetry nor low enough for economical direct image analysis.

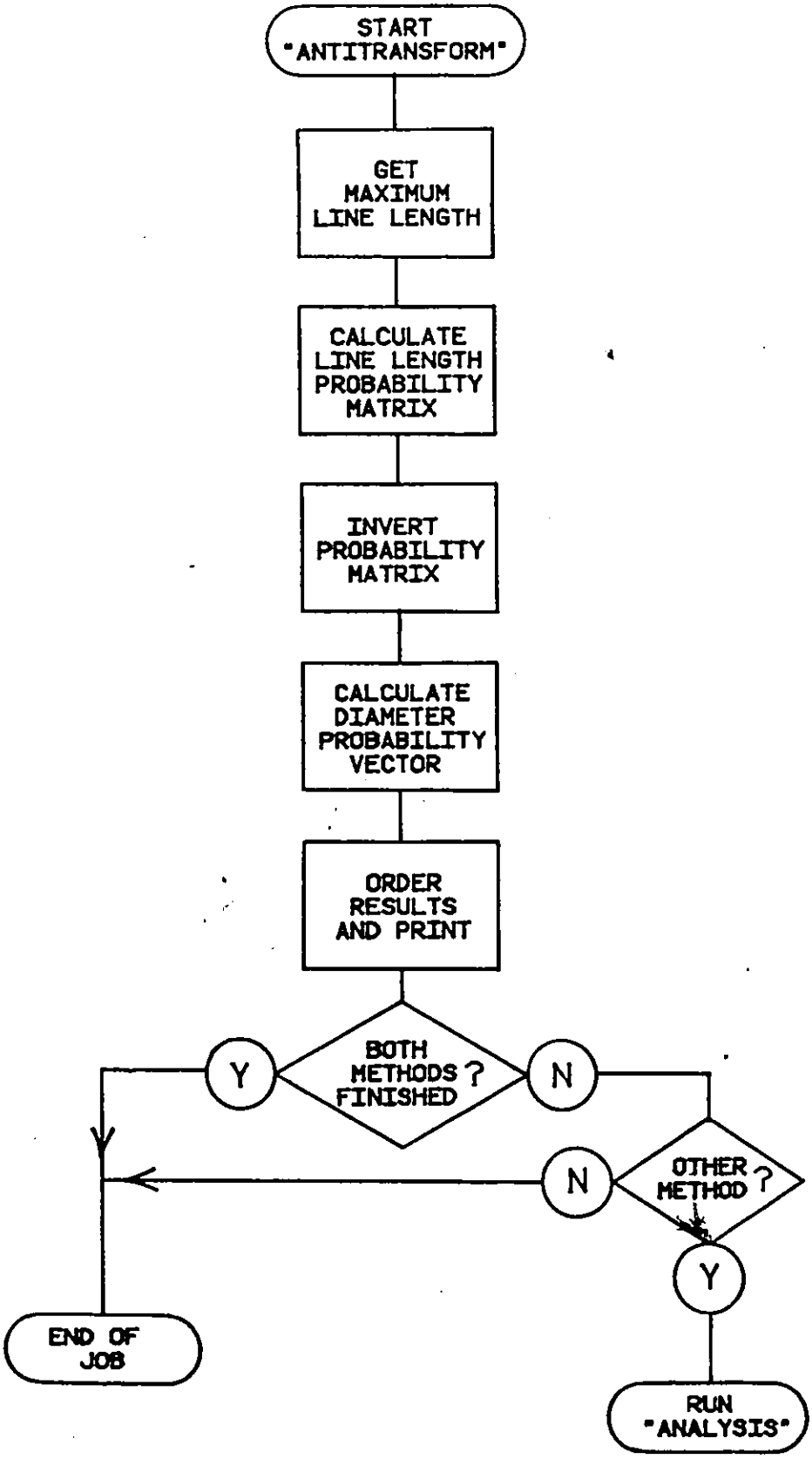
START "ANTITRANSFORM"
GET MAXIMUM LINE LENGTH
CALCULATE LINE LENGTH PROBABILITY MATRIX
INVERT PROBABILITY MATRIX
CALCULATE DIAMETER PROBABILITY VECTOR
ORDER RESULTS AND PRINT
BOTH METHODS FINISHED ?
Y
N
OTHER METHOD ?
N
Y
END OF JOB
RUN "ANALYSIS"

3) Display and controls:

Apart from the display subroutine used to display the image on the monitor screen, a program was written to display the distributions of total number of white pixels and of line length. "Histogram" displays the vector or its derivate, logarithmic or not, smoothed or not. The decisions about the kind of display are made through use of the Nova front panel switches.

Other switches allow the operator to stop program execution; in the default condition (all switches set to zero) the program will automatically run with no interruption until both methods of analysis have been finished.

CHAPTER 5

MEASUREMENTS AND DISCUSSION

To study the performance of the system, several patterns created with white circles of two diameters, 5/16" and 1/2", on a black paper examined at various distances by a Sony AVC-3260 camera (2:1 interlacing) were analysed using both methods.

Table 5.1 lists the image conditions; figs. 5.1 to 5.4 are photographs of the screen during processing; figs. 5.5 to 5.13 show reductions of the computer printouts; a condensation of the results is in table 5.2. Pixel dimensions are $1 \times \alpha$, where α is the transformation constant of formula 3.1.

The number of circles obtained from the line length antitransformation are within $.4\sqrt{N}$ of the actual value of N (e.g. a 4% error for 100 circles) for radii down to 1.5, i.e., a shape with an area of 7 pixels for a value of $\alpha = 1$. Below this radius, a complete normalization table is necessary and the error in the result increases. Using these error values, the number of circles of one radius is, in some runs, not equal to the actual value within the estimated experimental error, but the total number is. This is due to the fact that circles of only one radius were used in the image simulation which

provided an estimation of the errors. When analysing an image with circles of more than one radius, the deviations in the number of circles of each group is larger than the estimated value, but the total sum partially cancels the deviation.

Figure 5.1

Histogram of the number of white pixels as a function of the discrimination level for run #3. There are 256 discrimination levels; the step size is 4 and the vertical reference lines spacing is 50.

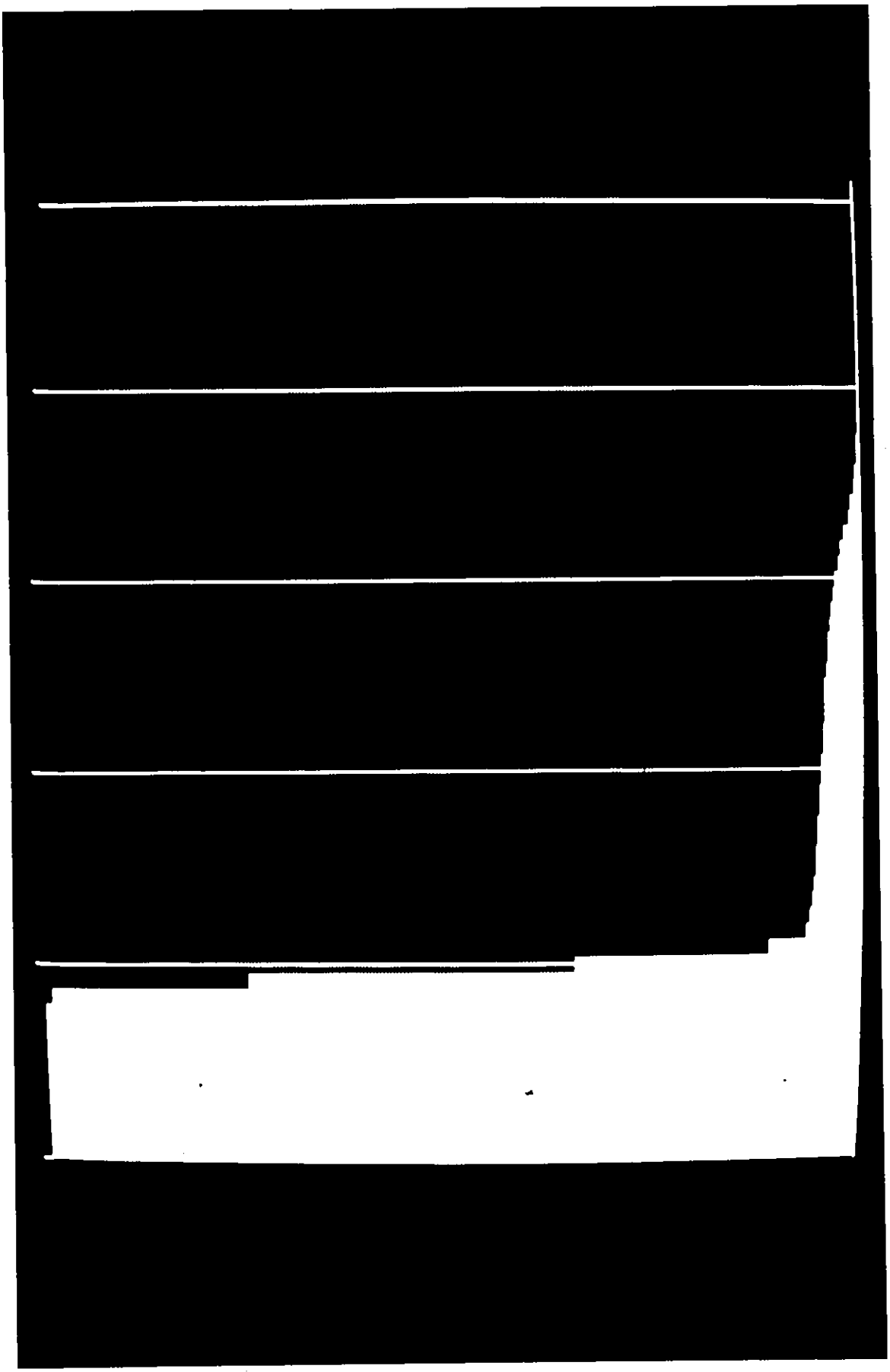

Figure 5.2

CRT screen after the optimum discrimination level has been calculated by "peak" showing the smoothed logarithmic grey level distribution function; the smoothing width is 32. The black vertical lines are in the position of the smoothed minimum and absolute maximum; the white vertical line indicates the value of the optimum discrimination level obtained from a least squares fit around the smoothed minimum. This value is used to obtain the digitized image displayed in the left lower quadrant of the screen.

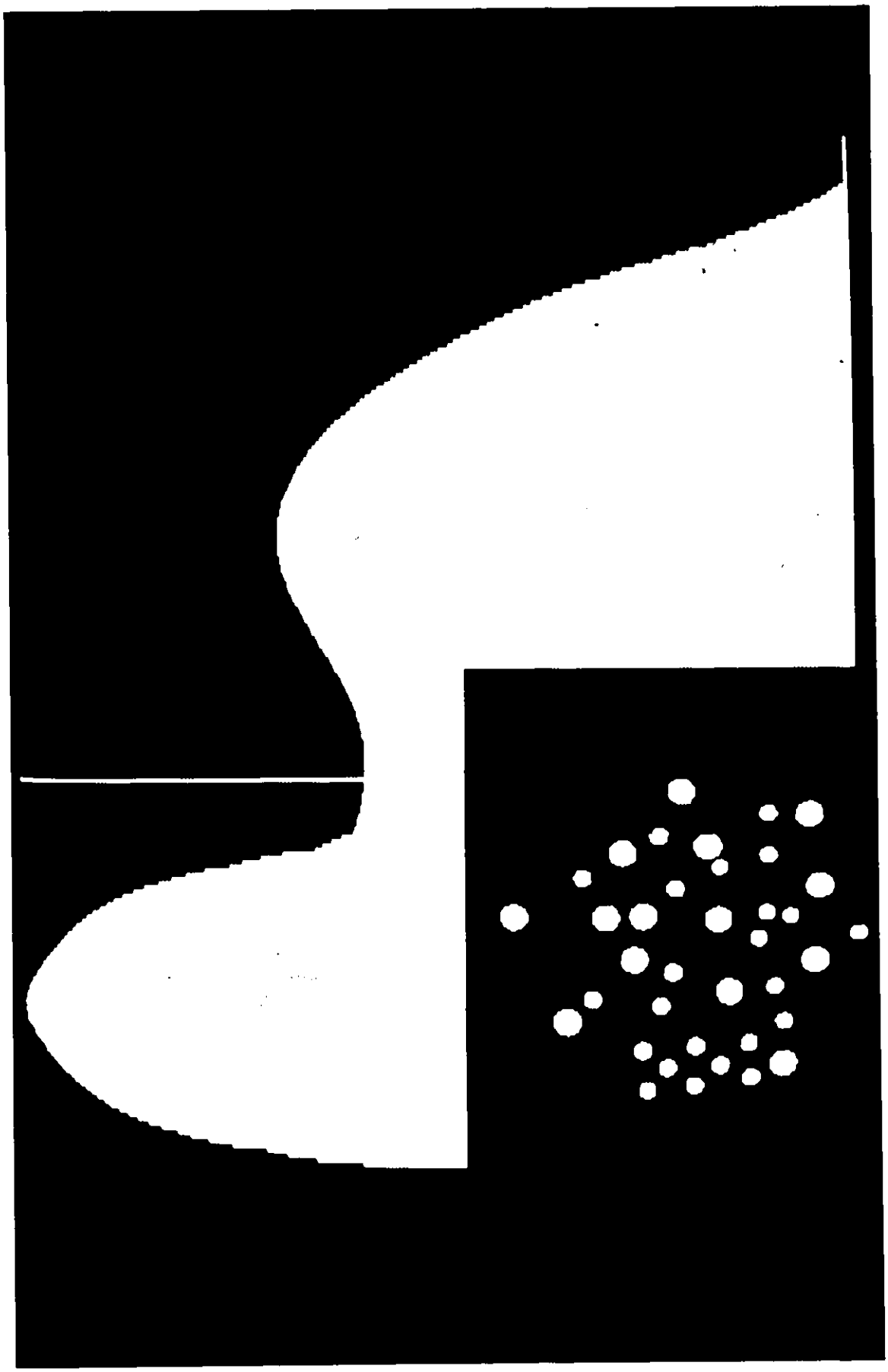

Figure 5.3

Image processing in operation: the four quadrants show, clockwise starting from the upper right side, the whole image, the processed figures, the present image and the last processed figure.

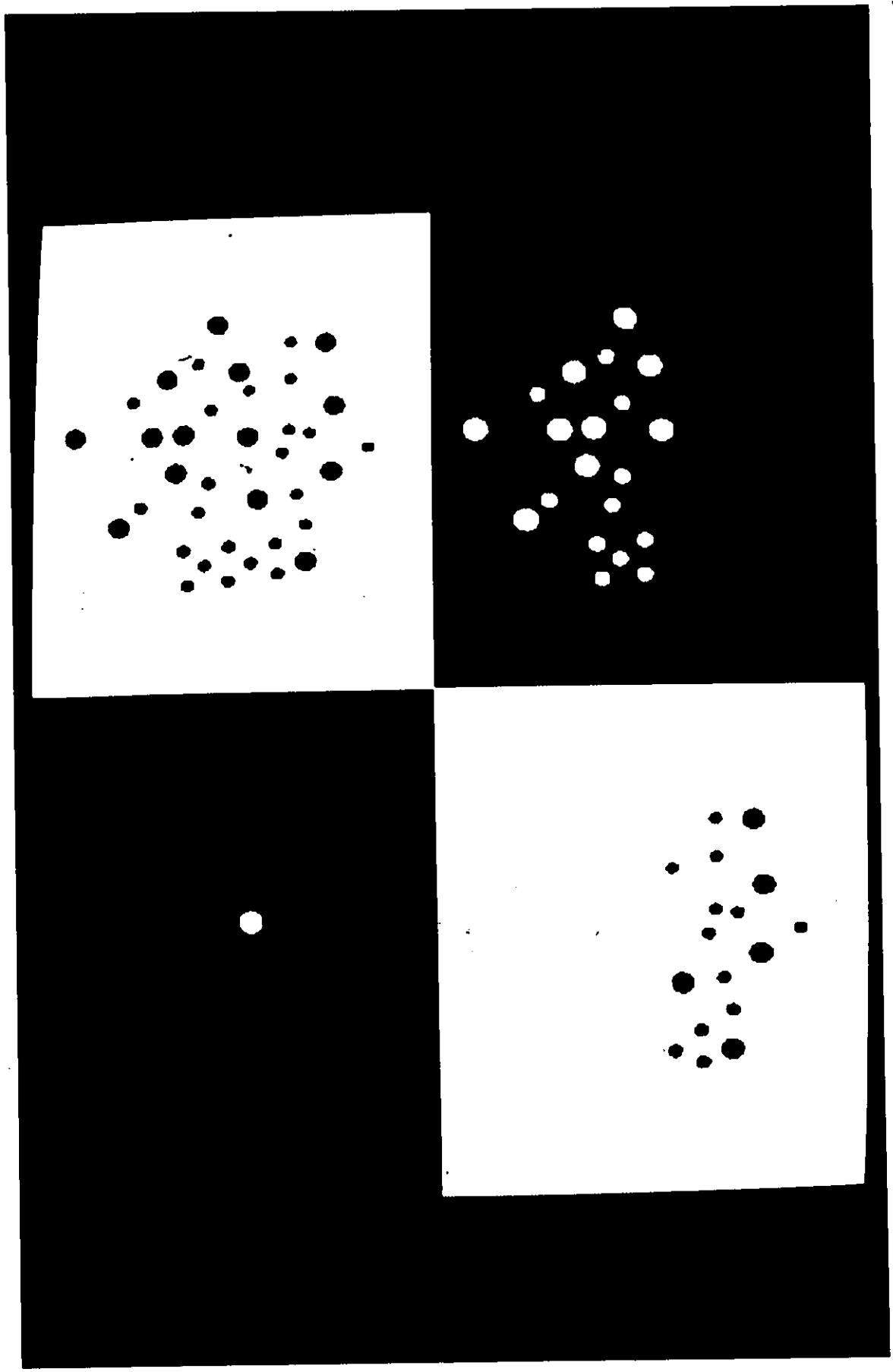

Figure 5.4

White line length distribution function corresponding to the digitized image of fig. 5.2. The histogram two peaks correspond to the two diameters of the circles used to generate the pattern. This function is antitransformed to obtain the number and radii of the circles on the image.

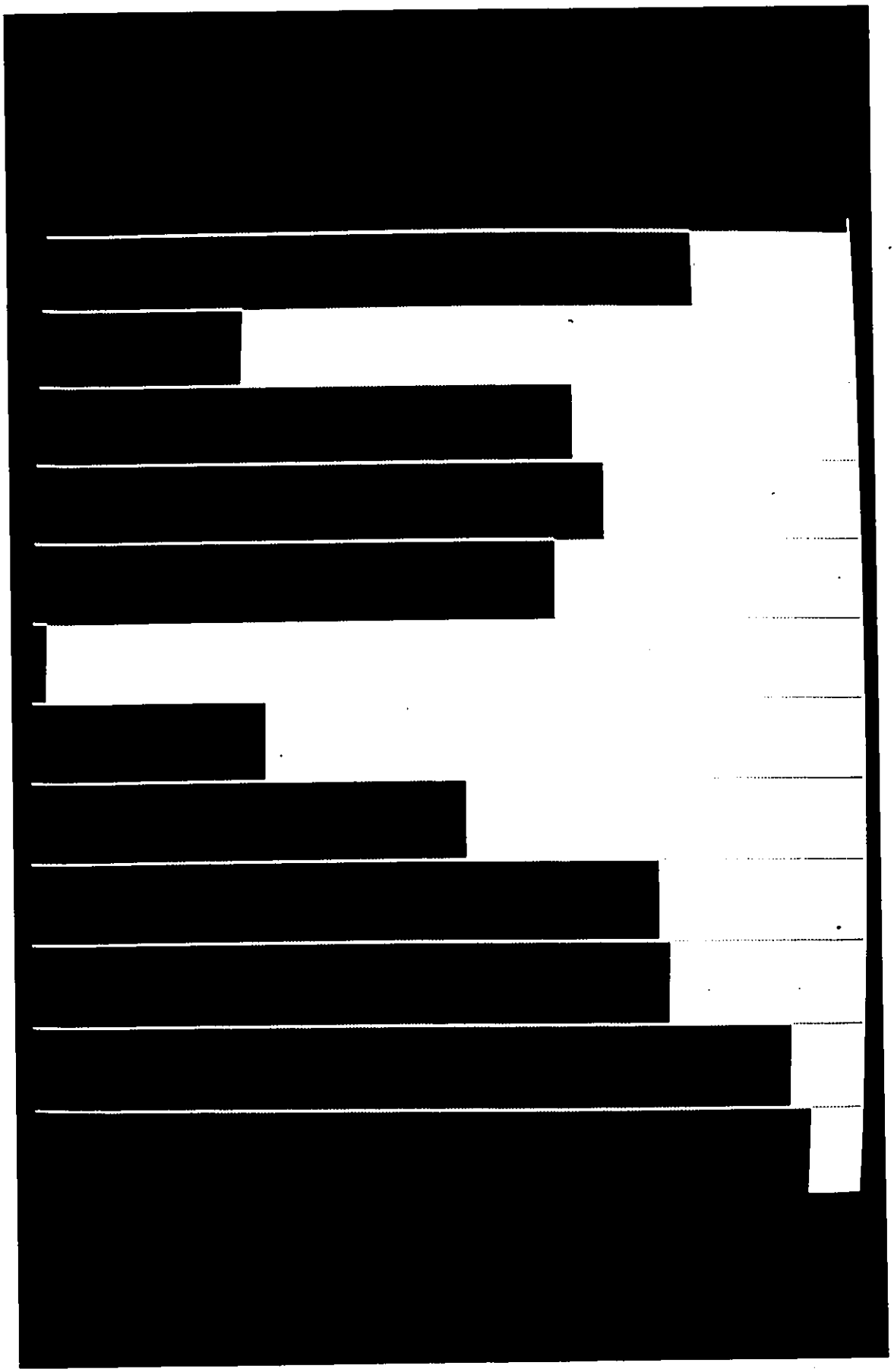

Run #	# of small circles	# of large circles	distance (cm)	Comments
1	36	0	200	
2	23	14	200	
3	23	14	90	Same pattern as in run #2
4	24	14	90	Added one small circle tangential to a large one with horizontal symmetry axis
5	24	14	90	Added one small circle tangential to a large one with vertical symmetry axis
6	5	8	30	

Table 5.1: List of images

Figure 5.5.

Run #1: Computer printout of both methods

```
*** IMAGE ANALYSIS ***
X CENTER      Y CENTER      RADIUS      ABS. ERROR
  52.1          140.0         1.78          .16
  58.6          111.1         1.71          .17
  59.6          128.0         1.78          .16
  60.6          156.3         1.63          .24
  63.9          118.9         1.71          .17
  65.3          143.9         1.55          .18
  67.6          104.2         1.86          .22
  72.0          111.9         1.71          .17
  72.1          136.0         1.78          .16
  71.7          165.5         1.46          .23
  75.3          120.1         1.71          .17
  78.6          151.1         1.71          .17
  81.7          140.0         1.71          .18
  82.9          107.5         1.78          .17
  86.2          116.4         1.86          .19
  86.2          129.5         1.78          .17
  88.7          139.5         1.78          .17
  89.3          160.0         1.63          .15
  92.6           96.1         1.78          .21
  92.2          126.1         1.71          .17
  93.8          148.2         1.63          .17
  97.2          113.7         1.78          .20
  99.6          162.8         1.63          .17
 101.3          106.0         1.78          .16
 103.6          140.9         1.71          .17
 104.6          153.2         1.63          .17
 105.3          128.7         1.78          .20
 107.4           93.1         1.78          .21
 111.0          137.0         1.63          .15
 112.2          118.4         1.86          .19
 116.9          162.9         1.55          .18
 120.3          101.6         1.86          .19
 121.3          124.5         1.78          .17
 122.1          146.5         1.78          .17
 124.6          135.8         1.63          .17
 128.3          152.5         1.46          .23

FINAL RESULTS
 RADIUS       # OF CIRCLES
   1.4              2
   1.6              9
   1.8             25
TOTAL NUMBER OF CIRCLES =    36

*** HISTOGRAM ***

*** ANTITRANSFORM ***
 RADIUS       # OF CIRCLES
   0.5             0.7
   1.0             9.0
   1.5            25.1
   2.0             6.9

FINAL RESULTS
 RADIUS       # OF CIRCLES       ERROR
   1.7            35.4             2.0
TOTAL NUMBER OF CIRCLES = 35.4 +/- 2.0

END OF JOB
```

Figure 5.6

Run #2: Computer printout of both methods.

*** IMAGE ANALYSIS ***

X CENTER	Y CENTER	RADIUS	ABS. ERROR
45.6	129.3	2.87	.22
55.0	102.5	3.00	.22
61.3	107.4	1.86	.19
62.0	137.1	1.71	.17
66.4	126.8	2.87	.23
71.7	116.0	2.87	.17
71.8	142.4	2.91	.20
71.7	83.7	1.93	.21
71.7	93.5	2.06	.13
74.8	126.4	2.96	.18
76.9	88.9	1.93	.22
76.7	104.3	1.93	.21
80.3	112.0	1.86	.21
80.3	145.9	1.71	.17
82.6	83.9	1.93	.25
82.9	132.5	1.78	.17
83.7	93.6	1.99	.20
86.2	156.1	2.73	.19
88.7	88.3	1.93	.18
90.9	142.2	2.96	.19
91.7	124.0	2.87	.17
92.5	106.2	2.96	.19
93.0	136.9	1.71	.17
95.8	84.5	2.06	.13
96.0	93.1	1.78	.21
100.4	118.4	1.71	.20
103.3	87.0	2.87	.17
102.9	106.0	1.78	.16
102.9	124.6	1.71	.20
104.4	97.5	1.93	.20
104.3	138.8	1.71	.22
104.6	149.0	1.78	.16
107.9	123.0	1.78	.16
112.4	111.6	2.91	.20
113.7	147.8	2.73	.20
114.8	130.0	2.77	.19
122.2	117.1	1.55	.18

FINAL RESULTS

RADIUS	# OF CIRCLES
1.6	1
1.8	13
2.0	9
2.8	8
3.0	6

TOTAL NUMBER OF CIRCLES = 37

*** HISTOGRAM ***

*** ANTITRANSFORM ***

RADIUS	# OF CIRCLES
0.5	-0.1
1.0	2.3
1.5	18.5
2.0	5.4
2.5	10.7
3.0	4.8

FINAL RESULTS

RADIUS	# OF CIRCLES	ERROR
2.8	17.8	1.4
1.6	21.7	1.8

TOTAL NUMBER OF CIRCLES = 39.4 +/- 2.3

END OF JOB

Figure 5.7

Run #3: Computer printout of both methods.

```
••• IMAGE ANALYSIS •••
X CENTER      Y CENTER      RADIUS      ABS. ERROR
  21.1          136.6         5.83          .22
  44.6           87.8         5.87          .20
  51.1          155.0         3.68          .19
  55.7           98.1         3.78          .19
  61.2          136.0         5.83          .19
  68.4          166.8         5.69          .21
  73.5          116.4         5.76          .22
  77.2          136.8         5.80          .20
  77.5           74.5         3.85          .18
  79.6           56.1         3.64          .19
  83.9          174.9         3.68          .27
  85.0           95.0         3.68          .15
  88.1           66.6         3.71          .22
  90.0          110.6         3.89          .18
  90.9          149.9         3.71          .17
  93.3          196.1         5.67          .22
  99.8           58.2         3.68          .20
 100.1           76.5         3.82          .20
 104.5          170.1         5.76          .18
 109.2          135.2         5.69          .20
 109.6          160.1         3.42          .19
 110.8           67.5         3.82          .20
 114.2          101.5         5.76          .22
 123.0           77.8         3.61          .19
 124.0           61.8         3.71          .20
 126.3          126.3         3.53          .19
 129.6          138.7         3.49          .19
 130.2          165.9         3.57          .18
 130.0          185.9         3.57          .20
 133.4          103.9         3.61          .18
 137.7           68.1         5.71          .19
 137.8           87.7         3.57          .23
 139.8          136.8         3.45          .21
 147.5          185.2         5.67          .21
 150.5          116.0         5.74          .18
 152.0          151.1         5.69          .20
 168.8          128.5         3.42          .19

FINAL RESULTS
 RADIUS       # OF CIRCLES
   3.4              4
   3.6             11
   3.8              8
   5.6              5
   5.8              9
TOTAL NUMBER OF CIRCLES =    37

••• HISTOGRAM •••

••• ANTITRANSFORM •••
 RADIUS       # OF CIRCLES
   0.5              1.9
   1.0             -1.3
   1.5              1.5
   2.0             -1.5
   2.5              1.6
   3.0              5.7
   3.5             14.8
   4.0              2.8
   4.5              1.2
   5.0              0.5
   5.5             10.2
   6.0              2.8

FINAL RESULTS
 RADIUS       # OF CIRCLES       ERROR
   5.7             12.8             1.2
   3.7             25.6             1.8
TOTAL NUMBER OF CIRCLES = 38.4 +/- 2.2

END OF JOB
```

Figure 5.8

Run #4: Computer printout of the results obtained using image analysis.

*** IMAGE ANALYSIS ***

X CENTER	Y CENTER	RADIUS	ABS. ERROR
21.3	133.9	7.04	1.59
44.6	87.8	5.92	.20
51.2	155.0	3.75	.20
55.6	98.1	3.75	.21
61.2	136.0	5.87	.18
68.4	166.7	5.80	.22
73.5	114.3	5.80	.22
77.3	136.7	5.87	.21
77.5	74.4	3.78	.22
79.7	56.1	3.71	.20
84.0	174.9	3.64	.25
85.0	95.0	3.68	.15
88.2	66.5	3.78	.21
90.0	110.5	3.85	.18
90.9	149.9	3.75	.18
93.3	196.1	5.67	.22
99.8	58.2	3.68	.20
100.0	76.4	3.89	.18
104.5	170.0	5.74	.19
109.2	135.3	5.78	.22
109.6	160.0	3.53	.19
110.8	67.5	3.82	.20
114.2	101.6	5.78	.21
123.0	77.8	3.61	.19
124.1	61.9	3.75	.18
126.3	126.2	3.61	.19
129.6	138.4	3.53	.21
130.1	165.9	3.61	.18
130.0	185.9	3.53	.21
133.4	103.9	3.64	.18
137.7	68.1	5.71	.19
137.6	87.8	3.61	.21
139.9	136.8	3.49	.20
147.5	185.2	5.67	.20
150.5	116.0	5.74	.18
152.0	151.1	5.74	.18
169.0	128.4	3.42	.25

FINAL RESULTS

RADIUS	# OF CIRCLES
3.4	2
3.6	11
3.8	10
5.6	2
5.8	10
6.0	1
7.0	1

TOTAL NUMBER OF CIRCLES = 37

END OF JOB

Figure 5.9

Run #4: Computer printout of the results obtained using line length distribution antitransformation.

*** HISTOGRAM ***

*** ANTITRANSFORM ***

RADIUS	# OF CIRCLES
0.5	2.4
1.0	0.5
1.5	0.3
2.0	-1.2
2.5	1.4
3.0	5.1
3.5	15.8
4.0	2.9
4.5	1.8
5.0	-0.7
5.5	9.5
6.0	3.5
6.5	-0.0
7.0	-0.0
7.5	-0.0
8.0	-0.1
8.5	-0.1
9.0	-0.1
9.5	0.5

FINAL RESULTS

RADIUS	# OF CIRCLES	ERROR
9.5	0.5	0.2
5.8	12.7	1.2
3.7	26.4	1.8

TOTAL NUMBER OF CIRCLES = 39.7 +/- 2.2

END OF JOB

Figure 5.10

Run #5: Computer printout of both methods.

```
*** IMAGE ANALYSIS ***
X CENTER      Y CENTER      RADIUS      ABS. ERROR
  24.1          136.7         7.01          1.76
  44.5           87.9         5.87           .19
  51.1          154.9         3.71           .20
  55.7           98.1         3.78           .19
  61.2          136.0         5.87           .18
  68.4          166.6         5.78           .21
  73.5          116.4         5.78           .21
  77.2          136.8         5.83           .21
  77.6           74.3         3.82           .21
  79.7           56.1         3.71           .20
  84.0          174.8         3.61           .26
  85.0           95.0         3.68           .15
  88.3           66.5         3.82           .20
  90.0          110.5         3.85           .18
  90.9          149.9         3.75           .18
  93.3          196.0         5.64           .21
  99.8           58.2         3.71           .21
 100.2           76.4         3.82           .20
 104.6          170.0         5.74           .19
 109.2          135.2         5.74           .22
 109.7          160.0         3.49           .18
 110.8           67.5         3.85           .18
 114.2          101.6         5.78           .21
 123.1           77.8         3.64           .19
 124.0           61.8         3.71           .20
 126.4          126.1         3.57           .19
 129.6          138.4         3.53           .21
 130.2          185.9         3.57           .18
 130.4          165.8         3.61           .19
 133.5          103.9         3.57           .18
 137.8           68.0         5.74           .18
 137.9           87.7         3.53           .21
 140.0          136.8         3.53           .20
 147.6          185.3         5.67           .22
 150.5          116.0         5.74           .18
 152.1          154.1         5.74           .19
 169.0          128.4         3.49           .25

FINAL RESULTS
 RADIUS       # OF CIRCLES
   3.4              2
   3.6             10
   3.8             11
   5.6              2
   5.8             11
   7.0              1
TOTAL NUMBER OF CIRCLES =    37

*** HISTOGRAM ***

*** ANTITRANSFORM ***
 RADIUS       # OF CIRCLES
   0.5             3.7
   1.0            -1.7
   1.5             0.3
   2.0            -0.2
   2.5             0.8
   3.0             5.4
   3.5            15.8
   4.0             3.2
   4.5             1.5
   5.0            -0.3
   5.5            10.4
   6.0             3.1

FINAL RESULTS
 RADIUS       # OF CIRCLES       ERROR
   5.7            13.1             1.2
   3.7            26.0             1.8
TOTAL NUMBER OF CIRCLES = 39.1 +/- 2.2

END OF JOB
```

Figure 5.11

Run #6: Computer printout of both methods.

```
*** IMAGE ANALYSIS ***
X CENTER      Y CENTER      RADIUS      ABS. ERROR
  27.2          164.8        18.31          .32
  26.1           39.8        11.39          .33
  33.6          121.8        11.55          .23
  53.4           77.6        17.95          .24
  59.4          206.0        11.46          .27
  66.1           21.0        11.27          .29
  76.3          118.5        11.19          .19
  89.1          151.6        11.44          .25
 113.5          191.4        18.10          .32
 109.3           95.2        11.26          .21
 137.0           38.1        17.65          .20
 154.0          123.8        18.13          .21
 164.6           74.5        11.37          .25

FINAL RESULTS
 RADIUS       # OF CIRCLES
  11.2              3
  11.4              4
  11.6              1
  17.6              1
  18.0              2
  18.2              1
  18.4              1
TOTAL NUMBER OF CIRCLES =    13

*** HISTOGRAM ***

*** ANTITRANSFORM ***
 RADIUS       # OF CIRCLES
   0.5             0.6
   1.0             0.1
   1.5            -0.1
   2.0            -0.5
   2.5             0.4
   3.0            -0.6
   3.5             0.3
   4.0             0.2
   4.5             0.1
   5.0             0.0
   5.5            -0.6
   6.0             0.6
   6.5            -0.8
   7.0             1.1
   7.5            -0.2
   8.0            -0.5
   8.5            -0.0
   9.0             0.4
   9.5            -0.2
  10.0             0.8
  10.5             0.0
  11.0             4.4
  11.5             2.4
  12.0             0.5
  12.5             0.1
  13.0            -0.3
  13.5             0.3
  14.0            -0.2
  14.5             0.1
  15.0            -0.1
  15.5             0.1
  16.0            -0.0
  16.5            -0.1
  17.0             0.6
  17.5             1.1
  18.0             3.2
  18.5             0.2

 FINAL RESULTS
  RADIUS       # OF CIRCLES      ERROR
   18.1             5.0            0.8
   11.4             8.4            1.0
 TOTAL NUMBER OF CIRCLES = 13.4 +/- 1.3

 END OF JOB
```

Run #	Image analysis		Antitransformation		
	Radius	# of circles	Radius	# of circles	Total # of circles
1	1.71±.03	36	1.7±.1	35.4±2.0	35.4±2.0
2	1.84±.03	23	1.6	21.7±1.8	39.5±2.3
	2.87±.05	14	2.8	17.8±1.4	
3	3.65±.04	23	3.7	25.6±1.8	38.4±2.2
	5.75±.05	14	5.7	12.8±1.2	
4	3.68±.04	23	3.7	26.4±1.8	39.6±2.2
	5.78±.05	12	5.8	12.7±1.2	
	7.0 ±1.6	1	9.5	.5± .2	
5	3.67±.07	23	3.2	26.0±1.8	39.1±2.2
	5.77±.06	13	5.7	13.1±1.2	
	7.0 ±1.8	1			
6	11.35±.08	8	11.4	8.4±1.0	13.4±1.3
	17.97±.11	5	18.1	5.0± .8	

Table 5.2: A condensation of the results obtained from both methods of analysis.

CHAPTER 6

CONCLUSIONS AND SUGGESTIONS

Both methods of image analysis have a different range of application: for films with low track density, a relatively small magnification is necessary to produce an image with a statistically meaningful number of holes; this means that the hole areas will be small rendering the antitransform method useless; also, in this case, the direct image analysis speed will be high due to the small number of white pixels to process.

For large track density, the magnification of the image can be increased, since a smaller field can provide the necessary precision thereby allowing use of the antitransformation method which will in this case be much faster than the direct image analysis. The antitransformation method requires a smaller computer memory and operates in real time: only one frame is needed to record the line length distribution function. The interface circuit must have an internal memory to store the distribution vector; after a frame is finished, the computer reads and processes it. Since the computer memory is not used to store the image, the accuracy of the system can be improved by increasing the horizontal and vertical resolution. As the bandwidth of good TV cameras is

of the order of 10 MHz the pixel clock frequency can be increased up to 20 MHz. Reading frames in which the time interval between the vertical and first horizontal syncronisation pulses changes would allow one to effectively increase the vertical resolution up to the scanning dot size. This could be accomplished using external syncronisation or, in cameras with random interlacing, by enabling the interface only in frames with the desired time difference.

In both cases, α (formula 4.1) must be modified accordingly to the new aspect ratio.

REFERENCES

1) J. E. Gingrich and J. C. Fisher, "Exploration for Uranium Utilizing the Track Etch Technique", 25th. International Geological Congress, Sydney (1976).

2) P. Duport, G. J. Madeleine and J. Pradel, "A Portable Dosimeter for Radon Daughter Products", Internal Report, French Atomic Energy Commission.

3) Canada Gazette Part II, 112, 406 (1974).

4) C. F. Williamson, J. P. Boujot and J. Picard, Tables of Range and Stopping Power for Charged Particles of Energy 0.5 to 500 Mev, Commisariat a l'Energie Atomique, France (1966).

5) R. Gold and C. E. Cohn, Rev. Sci. Instrum. 43, 18 (1972).

6) H. B. Luck, Radiation Effects 29, 205 (1976).

7) F. H. Ruddy, H. B. Knowles and G. E. Tripard, Phys. Rev. Letters 37, 826 (1976).

8) A. M. Chapuis, D. Dajlevic and M. Gerard-Nicodeme, Bulletin of the French Society for Radio Protection 4, 203 (1969).

9) H. B. Luck, Nucl. Instr. and Methods 124, 359 (1975).

10) A. Y. Qaqish and C. B. Besaret, Nucl. Instr. and Methods 138, 493 (1976).

11) R. Countess, "Quantitative Measurement of Alpha Activity Using Alpha Track-etch Film", Internal Report, Health and Safety Laboratory, U.S. Energy Research and Development Administration, New York (1976).

12) C. E. Cohn and R. Gold, Rev. Sci. Instrum. 43, 12 (1972).

13) D. Azimi-Garakani and J. G. Williams, Nucl. Instr. and Methods 147, 69 (1977).

14) Quantimet 720, Metals Research Corp., Cambridge, England.

15) Quantex DS12 and DS20, Quantex Corporation, San Carlos, California.

16) D. G. Fink, Television Engineering, McGraw, New York (1952).

17) Data General Corporation, Reference Manual 093-001099 (1975).

18) Data General Corporation, Reference Manual 093-000065 (1975).

19) C. K. Chow and T. Kaneko, "Boundary Detection of Radiographic Images by a Threshold Method", Frontiers of Pattern Recognition, Academic, New York (1972).

20) S. A. Dudani, "Region Extraction Using Boundary Following", Pattern Recognition and Artificial Intelligence, ed. C. H. Chen, Academic, New York (1976).

21) U. K. Pratt, Digital Image Processing, Wiley, New York (1978).